

LASER BEAMS DOI: 10.1070/QEL16088

Properties of vortex beams formed by an array of fibre lasers and their propagation in a turbulent atmosphere

V.P. Aksenov, V.V. Dudorov, V.V. Kolosov

Abstract. **Using a numerical simulation, we investigate the possibility of synthesising vortex laser beams with a variable orbital angular momentum by a hexagonal array of fibre lasers under a phase control of individual subapertures of the array. We report the requirements to the parameters of the device generating a vortex beam (number and size of subapertures, as well as their mutual arrangement). The propagation dynamics of synthesised vortex beams is compared with that of conventional Laguerre–Gaussian beams in free space and in a turbulent atmosphere. The spectral properties of the synthesised beam, represented as a superposition of different azimuthal modes, are determined during its propagation in free space. The energy and statistical parameters of the synthesised and Laguerre–Gaussian vortex beams are shown to coincide with increasing propagation distance in a turbulent medium.**

Keywords: *optical vortex beams, array of fibre lasers, beam combining, orbital angular momentum.*

1. Introduction

In recent decades, laser beams having an orbital angular momentum (OAM) [1–4] have attracted considerable attention due to their special properties that are important for many practical applications [5–10]. Because of the presence of the transverse circulation component of the Poynting vector [2], these kinds of beams are called vortex beams. In particular, the possibility of using optical vortices for encoding and transmitting information is being intensively studied [8, 9]. Generation of vortex beams has become a new branch of modern optical science, i.e. singular optics [11].

There are many approaches to the generation of vortex beams with controllable parameters, some of them having been tested experimentally. These methods involve producing vortex beams by a coherent superposition of vortex-free beams [12–15], direct formation of single or multiple vortex beams at the laser cavity output [16–20], or transformation of a Gaussian beam into a vortex beam out of the laser resonator. The transducer may be a spiral phase plate [21, 22], a diffraction phase hologram [23–25], a pair of cylindrical lenses [26], a Dammann zone plate [27] or a Moiré diffractive spiral phase plate [28], phase nanostructures [29] and single-axis crystals [30]. There are also methods for generating vortex light beams based on the use of the polarisation properties of the beam [31–34], as well as on the microresonator technologies [35–37].

The most common methods for producing vortex beams are associated with a laser beam passing through spiral phase plates, or with the use of spatial light modulators (PSMs). In this case, a particular spiral phase plate functions only at a single wavelength and does not allow for the tuning of the topological charge of the vortex. PSM-based devices can provide an arbitrary phase distribution; however, high-resolution PSMs are expensive and generate the desired phase distribution in the reflected light, which makes it impossible to make a compact experimental setup. In addition, liquid-crystal PSMs are sensitive to the polarisation of light, which reduces their efficiency and gives rise to problems when working with weak signals. Some methods for generating vortex beams involve computer-generated holograms or special diffraction gratings. However, they, in turn, are ineffective in generating beams with certain topological charges. Microresonator technologies have been developed for specialised applications and are not yet available for routine use.

The development of modern multiplexing optical communication technology based on the OAM requires the fabrication of high-speed devices to generate vortex beams with a tunable topological charge. The above-mentioned PSM-based methods are not sufficiently fast and usually ineffective in transformation of one type of the beam to another. They are capable of switching the beam OAM with a frequency of less than 1 kHz. Therefore, an urgent task is to develop new high-speed methods and devices for generating vortex laser beams. These devices should be compact and relatively inexpensive, and in some applications they should provide their operation at a high radiation intensity.

In this paper, we investigate the possibility of generating optical vortex beams with a variable OAM by an array of fibre lasers. The method involves the phase control of light from individual subapertures of a hexagonal array to create a phase incursion $2n\pi$ in going round the synthesised beam centre. In this case, use is made of exotic laser beam engineering based on coherent combining of beams from a fibre laser array [38]. It should be noted that the formation of optical beams on the basis of a coherent array of beams with radial arrangement has been discussed previously [39]. The main advantage of the proposed method for synthesising a vortex

V.P. Aksenov, V.V. Dudorov V.E .Zuev Institute of Atmospheric Optics, Siberian Branch, Russian Academy of Sciences, pl. Akad. Zueva 1, 634055 Tomsk, Russia; e-mail: dvv@iao.ru;
V.V. Kolosov V.E .Zuev Institute of Atmospheric Optics, Siberian Branch, Russian Academy of Sciences, pl. Akad. Zueva 1, 634055 Tomsk, Russia; Tomsk Scientific Center, Siberian Branch, Russian Academy of Sciences, prosp. Akademicheskii 10/4, 634055 Tomsk, Russia

Received 29 March 2016; revision received 17 May 2016
Kvantovaya Elektronika **46** (8) 726–732 (2016)
Translated by I.A. Ulitkin

beam is a possibility of fast (with a frequency greater than 10^9 Hz [40]) phase shift of subapertures providing a change in the OAM.

Without considering the technical implementation of the proposed system of the formation of vortex beams, we use a numerical simulation in this paper to examine the properties of the formation and propagation of vortex beams, synthesised from a various number of beamlets, in a turbulent atmosphere.

2. Model of a vortex beam

Due to the fact that the analysis of the classical Laguerre–Gaussian vortex beams has been widely discussed in the literature, the study of the propagation of synthesised vortex beams will be predominantly performed based on a comparison with the characteristics of the field of a Laguerre--Gaussian beam LG_m^l:

$$E(r,\varphi,z=0)=\left(\sqrt{2}\,\frac{r}{a}\right)^l L_m^l\left(\frac{2r^2}{a^2}\right)\exp\left(-\frac{r^2}{a^2}\right)\exp(\mathrm{i}l\varphi), \quad (1)$$

where $r=\sqrt{x^2+y^2}$ and $\varphi=\arctan(y/x)$ are the polar coordinates; a is the beam radius; m is the radial mode index (in this study it is assumed to be equal to zero); and l is the value of the topological charge.

The field of the synthesised vortex beam is the sum of the fields on the N_a subapertures of the fibre laser array:

$$E(x,y,z=0)=\sum_{sub=1}^{N_a}E_{sub}(x,y,z=0), \quad (2)$$

where

$$E_{sub}(x,y,z=0)=A_{sub}(x-x^c_{sub},y-y^c_{sub})\exp(\mathrm{i}l\varphi^c_{sub}); \quad (3)$$

$$A_{sub}(x,y)=\begin{cases}\exp\left(-\dfrac{x^2+y^2}{a^2_{sub}}\right), & x^2+y^2\leqslant a^2_{sub},\\ 0, & x^2+y^2>a^2_{sub};\end{cases} \quad (4)$$

$$\varphi^c_{sub}=\arctan\left(\frac{y^c_{sub}}{x^c_{sub}}\right); \quad (5)$$

x^c_{sub} and y^c_{sub} are the coordinates of the subapertutre centre; and a_{sub} is the subaperture radius. In the case of a hexagonal packing of beamlets, a central beamlet with the coordinates $x^c=0$ and $y^c=0$ is absent. In addition, when forming a synthesised beam from multiple rings of beamlets (N_a = 18, 36, 60 and so on), inner rings can be also missing. The propagation of synthesised and Laguerre–Gaussian beams is simulated by solving the parabolic wave equation [41]. An atmospheric turbulence is modelled by a set of phase screens with allowance for temporal changes in the refractive index [42].

The amplitude and phase distributions of the field of the beam for a topological charge $l=3$ are shown in Fig. 1. It can be seen that the number of subapertures constituting a synthesised vortex beam, similar to a continuous Laguerre–Gaussian beams, governs the radius of a single subaperture. Furthermore, with this method of forming the vortex beam it is obvious that the number of subapertures also determines the maximum possible value of the topological charge.

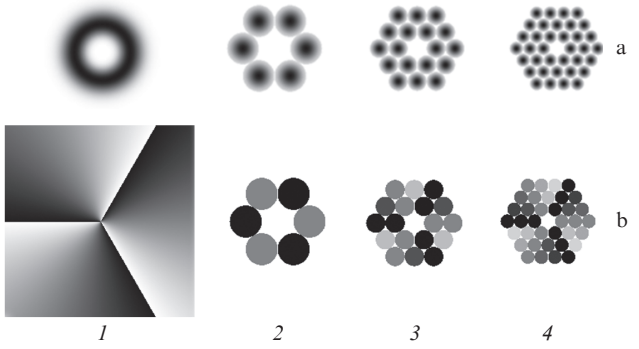

Figure 1. (a) Amplitude and (b) phase distributions of the fields of (*1*) Laguerre–Gaussian and (*2–4*) synthesised vortex beams with a topological charge $l=3$.

3. Characteristics of a synthesised vortex beam

3.1. Propagation in free space

Figure 2 shows the amplitude and phase distributions of the field of a synthesised vortex beam with a topological charge $l=3$ after it propagates in free space at a distance equal to half the diffraction length $L_d=ka^2$ (k is the wave number of the light), which corresponds to a continuous Laguerre–Gaussian beam. One can see that the field amplitudes and phases of the vortex beams synthesised from 18 or 36 subapertures behave, during the propagation, similarly to the case of a Laguerre–Gaussian beam: there is an annular distribution of the amplitude and a helical distribution of the phase with an incursion $2l\pi$ in going around the beam centre. However, during the propagation of a beam synthesised from six subapertures, the vortex component is not observed, and we can see only an interference pattern in the interaction of radiation from these apertures. This is obviously explained by the fact that the generation of a field with a nonzero orbital angular momentum l requires at least $3l$ sources of radiation. In this case, for a vortex beam with a topological charge $l=3$ to be formed, one should use at least nine subapertures arranged circumferentially.

In studying the influence of the structure of the synthesised beam (number of beamlet rings) on the formation of an optical vortex, we have found that the emission of the subapertures located in the inner rings of the fibre laser array has

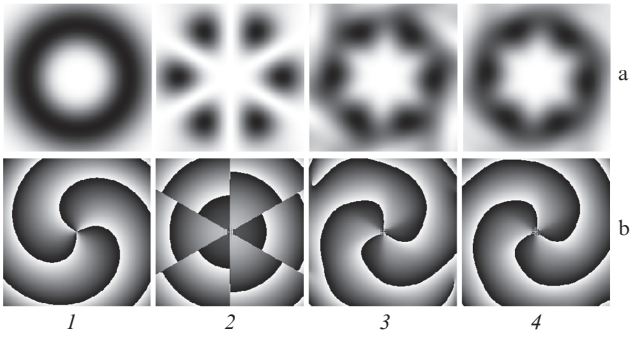

Figure 2. (a) Amplitude and (b) phase distributions of the fields of Laguerre–Gaussian and synthesised vortex beams presented in Fig. 1 during their propagation in free space at a distance $z=0.5ka^2$.

little effect on the formation of the OAM of the synthesised vortex beam. In this case, the maximum of the topological charge l_{max} is determined by the number of subapertures in the outer ring and does not depend on the number of the inner rings. It should also be noted that for the topological charge values close to l_{max}, the smoothed amplitude and phase distributions of the field are formed more rapidly (at smaller distances) in the presence of a single ring (when the inner rings are absent).

Figure 3 shows the amplitude and phase distributions of the field of the vortex beam synthesised by the fibre laser array consisting of three, two and one subaperture rings. One can see that in the case of free-space propagation the phase surface of the synthesised beams takes a characteristic spiral form, and the integral of the phase over a circle of radius $r_{max} = \langle \arg\max[A(r,\varphi)]\rangle_\varphi$ [$A(r,\varphi)$ is the field amplitude] is equal to 12π. Note, however, that this sufficiently smooth phase distribution of the field of the vortex beam synthesised by the fibre laser array is observed at some distance from the initial plane $z = 0$. In the initial part of the path, there is an interference of the fields of all subapertures of the fibre lasers, which does not allow one to determine correctly the OAM value of the synthesised beam.

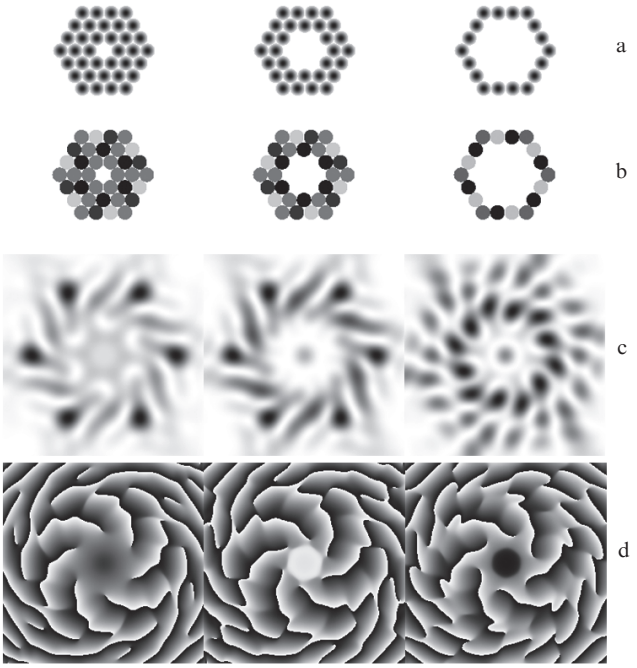

Figure 3. (a, c) Amplitude and (b, d) phase distributions of the field of the synthesised vortex beam with a topological charge $l = 6$ in the initial plane (a, b) and at a distance $z = 0.2ka^2$ (c, d).

Figure 4 shows the dynamics of the amplitude and phase distributions of the fields of Laguerre–Gaussian and synthesised beams propagating in free space. One can see that at the initial stage of propagation, the distribution of the field amplitude exhibits periodic structures, to which the distortions of the helical phase surface correspond. Then, due to diffraction the phase of the synthesised field, whose amplitude distribution takes a continuous ring-shaped appearance, is smoothed. It should be noted that the continuous (smoothed) phase distribution is formed much earlier than a uniform annular distribution of the field amplitude. At the same time, at a sufficiently large distance from the transmitter system (in this case, for $z > 0.5ka^2$), the amplitude and phase distributions of the field of the synthesised beam virtually coincide with the corresponding distributions for a Laguerre–Gaussian beam.

Note that in the case of a hexagonal packing of the synthesised vortex beam at a topological charge l multiple of six, one can observe a rotational symmetry in the distribution of both amplitude and phase of the field. For values of l, not multiples of six, there is a distortion of the symmetry of the phase distribution. Figure 5 shows the amplitude and phase distributions of the field of the vortex beam synthesised from 36 subapertures with different values of the topological charge. It can be seen that the distribution of the radiation intensity, regardless of l, always exhibits a hexagonal symmetry. In the field phase distribution for $l = 1-3$ a single dislocation point is formed on the optical axis. In this case, the phase incursion in the integration along the contour passing through local maxima of the field intensity around the centre point is $2l\pi$. For $l = 4$, 5 (not multiple of six), six hexagonally (symmetrically) arranged dislocation points of the wavefront are formed, as well as one (for $l = 5$) or two (for $l = 4$) additional dislocation points of an 'opposite sign' on the optical axis. Thus, in this case, the phase incursion in the integration along the contour passing through the local maxima of the field intensity around the centre point is also equal to $2l\pi$. For $l = 6$, six hexagonally arranged dislocation points of the wavefront are formed, which in the integration along the contour passing through the local maxima of the field intensity also provide a phase incursion equal to $2l\pi$.

It is obvious that the interference field structure of the synthesised vortex beam in the initial part of the propagation path will introduce distortions in the OAM. The effect of the nonuniform field structure of the synthesised beam on its characteristics can be evaluated by using an expansion of the field in the azimuthal modes of the vortex beam:

$$E(r,\varphi,z) = \frac{1}{\sqrt{2\pi}} \sum_{n=-\infty}^{\infty} a_n(r,z)\exp(in\varphi), \tag{6}$$

$$a_n(r,z) = \frac{1}{\sqrt{2\pi}} \int_0^{2\pi} d\varphi E(r,\varphi,z)\exp(-in\varphi). \tag{7}$$

Then, to identify the topological charge of the synthesised vortex beam we should calculate the fraction of the energy corresponding to different-order modes n:

$$P_n(z) = \frac{c_n(z)}{\sum_{i=-\infty}^{\infty} c_i(z)}, \tag{8}$$

where

$$c_n(z) = \int_0^{\infty} r dr\, |a_n(r,z)|^2. \tag{9}$$

Figure 6 shows the energy dynamics of the modes P_n of the synthesised vortex beam with a topological charge $l = 1$. In view of the restrictions used in the numerical simulations, we have performed the decomposition of ten modes ($n = -3 \div +6$). It can be seen that in contrast to a conventional vortex beam, for which all the energy is concentrated in the fundamental mode of the order of l, the propagation of the

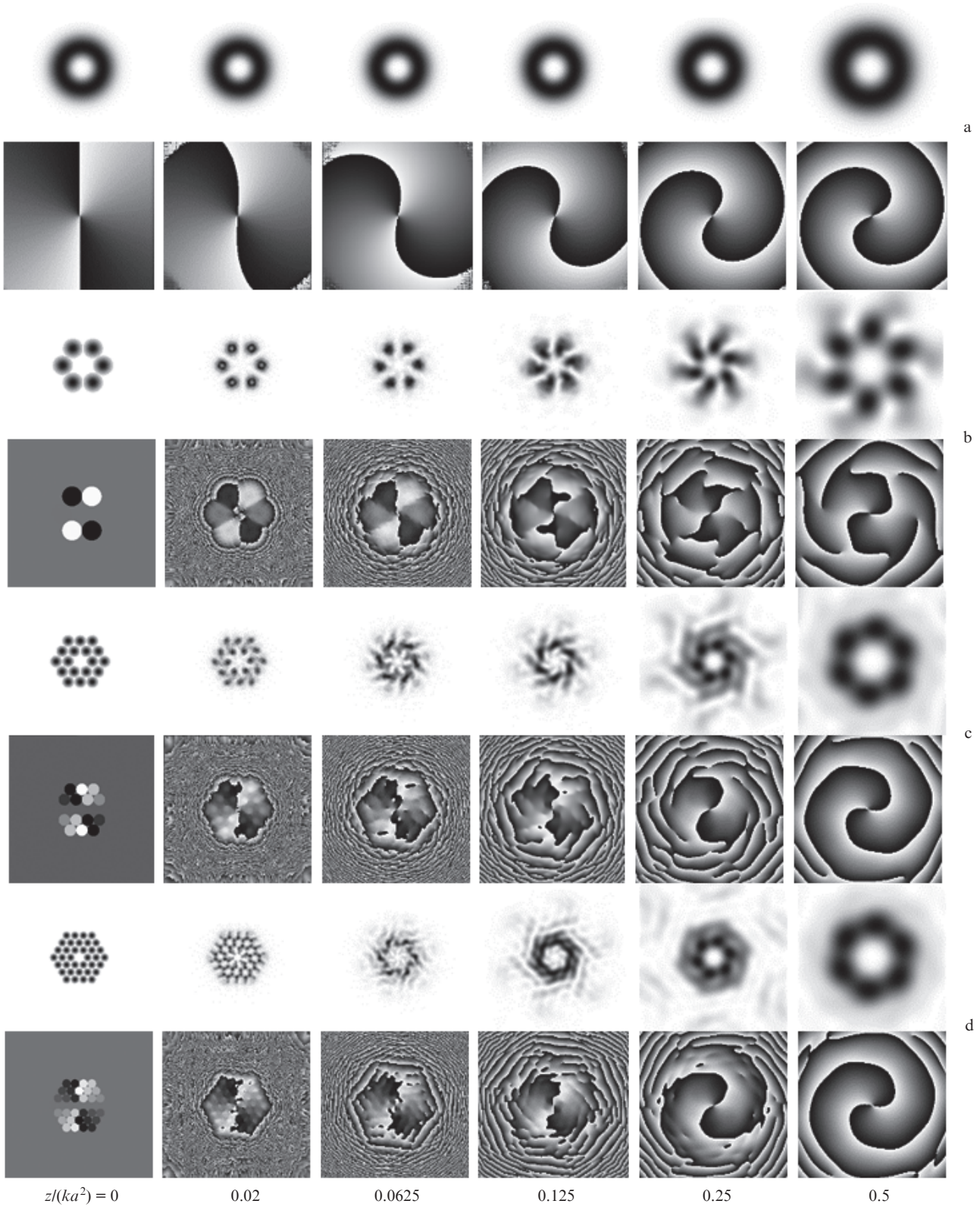

Figure 4. Dynamics of the amplitude and phase distributions of the fields of (a) Laguerre–Gaussian and (b–d) synthesised vortex beams ($l = 2$) during their propagation in vacuum.

synthesised beam at the initial part of the path is accompanied by an energy transfer between the modes with different values of n. In the initial plane, 50% of the energy is contained in the vortex-free zero-order mode. Then, as the beam propagates, the energy of the mode with $n = 1$, whose order is equal to the given topological charge $l = 1$, increases sharply to 60%, and after it again decreases down to 10%–30% at point $z = 0.125ka^2$ corresponding to the minimum of the effective size of the synthesised beam. Upon further beam propagation, the energy of the mode with $n = 1$ increases monotoni-

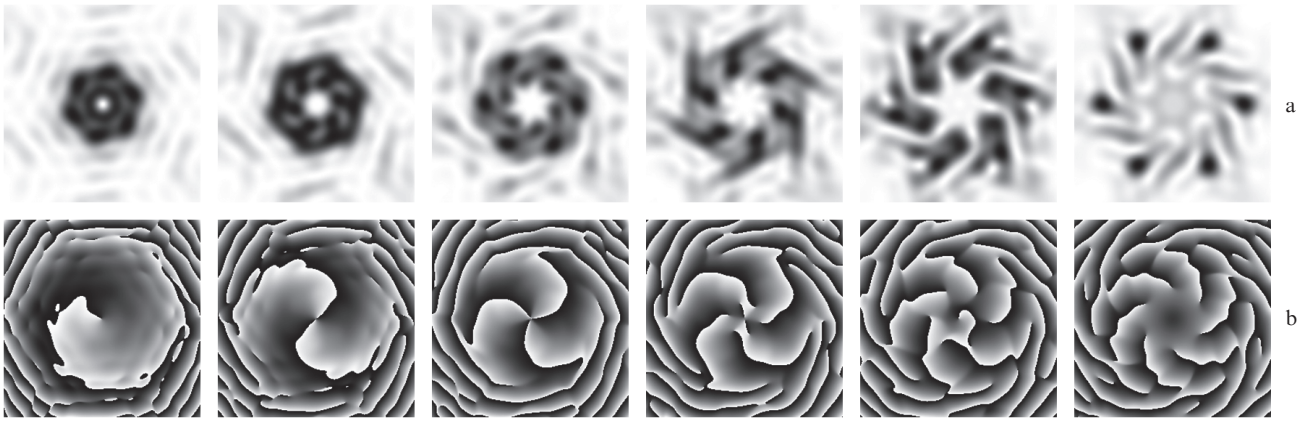

Figure 5. (a) Amplitude and (b) phase distributions of the field of the synthesised vortex beam from 36 subapertures at a distance $z = 0.2ka^2$ for different values of the topological charge.

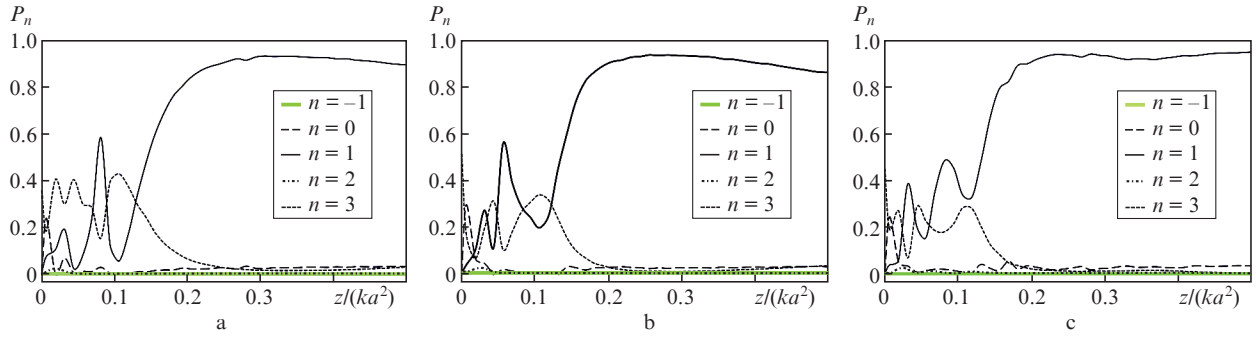

Figure 6. Dynamics P_n of the synthesised vortex beam propagating in free space and having a topological charge $l = 1$ at N_a = (a) 6, (b) 18 and (c) 36.

cally and saturates at a level of 90%–95%. A similar behaviour of the mode composition of the synthesised beam is observed for other values of the topological charge. Thus, when the synthesised vortex beam propagates a distance $z > 0.2ka^2$, its properties begin to coincide with those of the Laguerre–Gaussian beam.

4. Propagation in a turbulent atmosphere

In applications related to the propagation of vortex beams in the atmosphere, an important issue in the case of generation of beams by a fibre laser array is the study of the propagation of these beams through turbulent inhomogeneities [43–45]. Figure 7 shows the results of calculation of the radiation intensities of synthesised vortex beams and a classical Laguerre–Gaussian beam. It can be seen that the distribution of the average intensity of the synthesised beams and a Laguerre–Gaussian beam virtually coincide. In this case, the intensity fluctuation dispersion decreases with increasing number of beamlets, which form a vortex beam, and approaches the values corresponding to a Laguerre–Gaussian beam.

Figure 8 illustrates the probability density function of the radiation intensity of the synthesised vortex beam and the Laguerre–Gaussian beam at several points across the beam cross sections. It is seen that the dependence is mainly determined by the average value of the radiation intensity at a given point and is virtually independent of where it is located (at the beam centre or at its periphery). One can also note that the probability density function for the Laguerre–Gaussian and synthesised beams at the given parameters of the problem is almost identical. This suggests that the propagation of the synthesised vortex beams in a turbulent medium in the conditions when the energy of the mode, the order of which is equal to a specified topological charge, becomes maximum, is similar to the propagation of traditional vortex beams with a continuous field distribution.

5. Conclusions

Thus, the method proposed in this paper allows one to synthesise vortex beams with a controlled OAM. It is shown that the maximum value of the topological charge l_{max} of the synthesised beam with a hexagonal packing is determined by the number of subapertures in the outer ring and does not depend on the number of subapertures in the inner ring. In addition, for a topological charge close to l_{max}, the formation of the smoothed amplitude and phase distribution of the field is faster (at smaller distances) in the presence of a single ring (when the inner rings are absent).

During the propagation of the synthesised beam at the initial part of the path, there is a transfer of energy between the azimuthal different-order modes. In the initial plane, the main part of the energy is contained in the vortex-free zero-order mode. Then, upon further propagation of the beam, the energy of the mode, the order of which is equal to the given topological charge, increases (in most cases, nonmonotonically) and saturates at a level of 90%–95%.

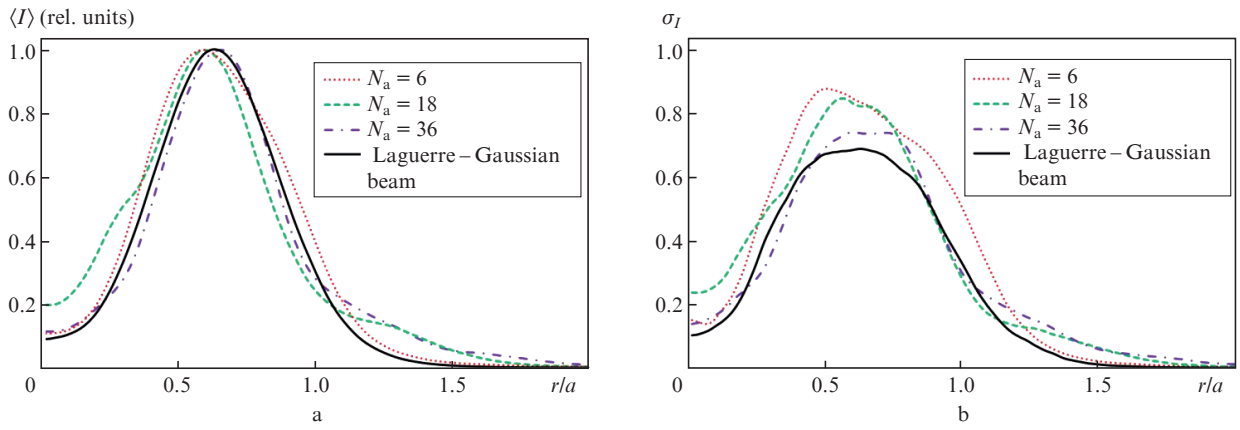

Figure 7. Average intensity distributions $\langle I\rangle$ and the standard deviation σ_I at $l = 1$, $z = 0.1ka^2$ and $D/r_0 = 4$ [$D = 2a$ is the beam diameter, and $r_0 = (0.423k^2C_n^2z)^{-3/5}$ is the Fried parameter, where C_n^2 is the structural characteristics of the refractive index of the turbulent atmosphere].

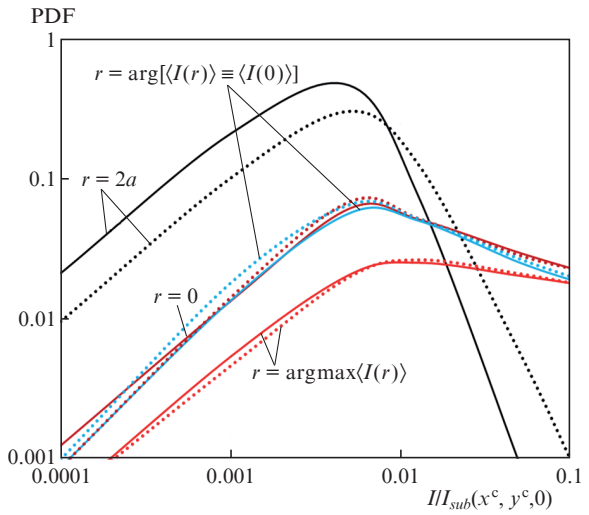

Figure 8. (Colour online) Probability density function (PDF) of the radiation intensity I of the synthesised (dashed curves) and Laguerre–Gaussian (solid lines) vortex beams at $z = 0.5ka^2$, $D/r_0 = 4$.

The propagation of such beams in a turbulent atmosphere is similar to that of well-studied vortex beams with a continuous field distribution. It is shown that the statistical characteristics of the synthesised vortex beams propagating through turbulent inhomogeneities almost coincide with those of Laguerre–Gaussian beams. It should be noted that the probability density function of the radiation intensity of the synthesised vortex beam on the axis coincides with the probability density function of the radiation intensity at the periphery of the beam with the same average value.

Acknowledgements. The work was supported by the Applied Research of the Ministry of Education and Science of the Russian Federation (Agreement No. 14.613.21.0035 dated 5 November 2015).

References

1. Jackson J.D. *Classical Electrodynamics* (New York–London: John Wiley & Sons, Inc., 1962; Moscow: Mir, 1965).
2. Allen L., Beijersbergen M.W., Spreeuw R.J.C., Woerdman J.P. *Phys. Rev. A*, **45**, 8185 (1992).
3. Franke-Arnold S., Allen L., Padgett M.J. *Laser Photonics Rev.*, **2**, 299 (2008).
4. Torres J.P., Torner L. *Twisted Photons* (Weinheim: Wiley-VCH, 2011).
5. Yao A.M., Padgett M.J. *Adv. Opt. Photon.*, **3**, 161 (2011).
6. Friese M.E.J., Enger J., Rubinsztein-Dunlop H., Heckenberg N.R. *Phys. Rev. A*, **54**, 1593 (1996).
7. Fickler R., Lapkiewicz R., Plick W.N., Krenn M., Schae C., Ramelow S., Zeilinger A. *Science*, **338**, 640 (2012).
8. Wang J., Yang J.Y., Fazal I.M., Ahmed N., Yan Y., Huang H., Ren Y., Yue Y., Dolinar S., Tur M., Willner A.E. *Nat. Photonics*, **6**, 488 (2012).
9. Willner A.E., Huang H., Yan Y., Ren Y., Ahmed N., Xie G., Bao C., Li L., Cao Y., Zhao Z., Wang J., Lavery M.P.J., Tur M., Ramachandran S., Molisch A.F., Ashrafi N., Ashrafi S. *Adv. Opt. Photon.*, **7**, 66 (2015).
10. Volostnikov V.G., Kotova S.P., Losevskii N.N., Rakhmatulin M.A. *Kvantovaya Elektron.*, **32**, 565 (2002) [*Quantum Electron.*, **32**, 565 (2002)].
11. Soskin M.S., Vasnetsov M.V., in *Progress in Optics* (Amsterdam: Elsevier, 2001).
12. Wang L.G., Wang L.Q., Zhu S.Y. *Opt. Commun.*, **282**, 1088 (2009).
13. Brignon A. *Coherent Laser Beam Combinin* (Weinheim: Wiley-VCH, 2013).
14. Vaity P., Aadhi A., Singh R.P. *Appl. Opt.*, **52**, 6652 (2013).
15. Zhang Z., Ye Z., Song D., Zhang P., Chen Z. *Appl. Opt.*, **52**, 8512 (2013).
16. Vaughan J.M., Willetts D.V. *J. Opt. Soc. Am.*, **73**, 1018 (1983).
17. Lee A.J., Zhang C., Omatsu T., Pask H.M. *Opt. Express*, **22**, 5400 (2014).
18. Kano K., Kozawa Y., Sato S. *Int. J. Opt.*, **2012**, 359141 (2012).
19. Senatsky Y., Bisson J.F., Li J., Shirakawa A., Thirugnanasambandam M., Ueda K.I. *Opt. Rev.*, **19**, 201 (2012).
20. Li H., Phillips D.B., Wang X., Ho Ying-Lung D., Chen L., Zhou X., Zhu J., Yu S., Cai X. *Optica*, **2**, 547 (2015).
21. Beijersbergen M.W., Coerwinkel R.P.C., Kristensen M., Woerdman J.P. *Opt. Commun.*, **112**, 321 (1994).
22. Starikov F.A., Kochemasov G.G., Koltygin M.O., Kulikov S.M., Manachinsky A.N., Maslov N.V., Sukharev S.A., Aksenov V.P., Izmailov I.V., Kanev F.Yu., Atuchin V.V., Soldatenkov I.S. *Opt. Lett.*, **34**, 2264 (2009).
23. Bazhenov V.Yu., Vasnetsov M.V., Soskin M.S. *Pis'ma Zh. Eksp. Teor. Fiz.*, **52**, 1037 (1990).
24. Heckenberg N.R., McDuff R., Smith C.P., White A. *Opt. Lett.*, **17**, 221 (1992).
25. Mirhosseini M., Magaña-Loaiza O.S., Chen C., Rodenburg B., Malik M., Boyd R.W. *Opt. Express*, **21**, 30196 (2013).
26. Beijersbergen M.W., Allen L., van der Veen H., Woerdman J.P. *Opt. Commun.*, **96**, 123 (1993).
27. Yu J., Zhou C., Jia W., Hu A., Cao W., Wu J., Wang S. *Appl. Opt.*, **51**, 6799 (2012).

28. Harm W., Bernet S., Ritsch-Marte M., Harder I., Lindlein N. *Opt. Express*, **23**, 413 (2015).
29. Srimathi I.R., Li Y., Delaney W.F., Johnson E.G. *Opt. Express*, **23**, 19056 (2015).
30. Paranin V.D., Karpeev S.V., Khonina S.N. *Kvantovaya Elektron.*, **46**, 163 (2016) [*Quantum Electron.*, **46**, 163 (2016)].
31. Oemrawsingh S., van Houwelingen J., Eliel E., Woerdman J.P., Verstegen E., Kloosterboer J., Hooft G. *Appl. Opt.*, **43**, 688 (2004).
32. Marrucci L., Karimi E., Slussarenko S., Piccirillo B., Santamato E., Nagali E., Sciarrino F. *J. Opt.*, **13**, 064001 (2011).
33. Asano M., Takahashi T. *Opt. Express*, **23**, 27998 (2015).
34. Gecevičius M., Drevinskas R., Beresna M., Kazansky P.G. *Appl. Phys. Lett.*, **104**, 231110 (2014).
35. Cai X., Wang J., Strain M.J., Morris B.J., Zhu J., Sorel M., O'Brien J.L., Thompson M.G., Yu S. *Science*, **338**, 363 (2012).
36. Strain M.J., Cai X., Wang J., Zhu J., Phillips D.B., Chen L., Lopez-Garcia M., O'Brien J.L., Thompson M.G., Sorel M., Yu S. *Nat. Commun.*, **5**, 4856 (2014).
37. Wang Y., Feng X., Zhang D., Zhao P., Li X., Cui K., Liu F., Huang Y. *Scientific Reports*, **5**, 10958 (2015).
38. Lachinova S.L., Vorontsov M.A. *J. Opt.*, **15**, 105501 (2013).
39. Wang L.G., Wang L.Q., Zhu S.Y. *Opt. Commun.*, **282**, 1088 (2009).
40. Vorontsov M.A., Lachinova S.L. *J. Opt. Soc. Am. A*, **25**, 1949 (2008).
41. Rytov S.M., Kravtsov Yu.A., Tatarskii V.I. *Principles of Statistical Radiophysics, Vol. 4: Wave propagation through Random Media* (Berlin: Springer-Verlag, 1989).
42. Dudorov V.V., Kolosov V.V., Filimonov G.A. *Proc. SPIE Int. Soc. Opt. Eng.*, **6160**, U170 (2005).
43. Aksenov V.P., Pogutsa Ch.E. *Kvantovaya Elektron.*, **38**, 343 (2008) [*Quantum Electron.*, **38**, 343 (2008)].
44. Aksenov V.P., Pogutsa Ch.E. *Opt. Atmos. Okeana*, **25**, 561 (2012) [*Atm. Ocean. Opt.*, **26**, 13 (2013)].
45. Falits A.V. *Opt. Atmos. Okeana*, **28**, 763 (2015).